



Trans. Nonferrous Met. Soc. China 33(2023) 765-776

Transactions of Nonferrous Metals Society of China

www.tnmsc.cn



Microstructure and properties of magnesium/steel dissimilar metals by interlayer assisted laser welding

Tao TAO^{1,2}, Jin-shui LIU^{1,2}, Dian-wu ZHOU², Hui-ming LI², Xin-yu WANG²

 College of Materials Science and Engineering, Hunan University, Changsha 410082, China;
 State Key Laboratory of Advanced Design and Manufacturing for Vehicle Body, Hunan University, Changsha 410082, China

Received 26 October 2021; accepted 28 March 2022

Abstract: The experiments of laser welding were carried out for AZ31B magnesium alloy and DP590 dual-phase steel in an overlap magnesium-on-steel configuration with interlayer addition. The interlayer elements were selected based on the calculation of thermodynamic properties and intrinsic mechanical properties, and the changes of microstructure and properties of magnesium/steel joint were analyzed. The results showed that with the addition of Sn and Al interlayers, the maximum load of the joint was 730 and 590 N, respectively, which was 2.04 times and 1.46 times higher than that without interlayer. With the addition of Al interlayer, the brittle Mg₁₇Al₁₂ compound was formed at the magnesium/steel interface, which limited the improvement of the mechanical performance of magnesium/steel joint. In the case of adding Sn interlayers, Mg₂Sn with relatively low brittleness and Fe₃Sn with a certain ductility were formed at the magnesium/steel interface, which was a vital reason that the properties of joint with Sn interlayer were higher than those with Al interlayer.

Key words: dissimilar metal welding; intermetallic compounds; mechanical properties; Sn powder, Al powder

1 Introduction

To solve the problems of increasingly serious energy crisis and environmental pollution, the application of light-weight alloys to partially or even totally substitute high density metals had attracted the attention of all countries in the world [1]. Magnesium alloy had low density and high specific strength [2], and steel was the most widely used material in modern transportation. The use of magnesium alloys to replace some steel could significantly reduce the mass of structural components [3]. Therefore, it was of great practical significance to realize the effective connection between magnesium alloys and steel. However, the physical and chemical properties of magnesium and steel were remarkably diverse. Meanwhile, Mg and

Fe were almost insoluble, it was difficult to form an interface layer at Mg/Fe interface, so the metallurgical connection between them could not be achieved [4].

Up to now, various welding techniques had been used for steel and magnesium alloys to achieve effective metallurgical connection by adding alloying elements [5–13]. LI et al [14] studied the influence of zinc coating on the interface reaction of magnesium alloy and steel laser brazing joints and the mechanical properties of the joints, and they found that the presence of zinc coating promoted the wetting and spreading of the liquid filler wire on steel base metal. LIU et al [15] carried out the hybrid laser-TIG welding by adding Cu foil between low carbon steel and magnesium alloy, the metallurgical connection of the joint was realized. ZHAO et al [16] provided the influence of

the Ni interlayer on the microstructure evolution in magnesium/steel laser brazing, and they found that the formation of FeAl, AlNi and Mg2Ni eutectic phases realized metallurgical bonding of the joint. ZHOU et al [17] conducted a laser welding experiment of adding an aluminum intermediate layer to two-way steel and AZ31 magnesium alloy, and they found that under appropriate laser power, a double molten pool structure generated on the joint, and AlFe, Al₂Fe and AlFe₃ were formed at interface to promote the metallurgical bonding between the upper and lower molten pools. NASIRI et al [12] pointed out that Fe(Al) solid solution and Al₈(Mn,Fe)₅ IMCs were formed at magnesium/steel interface, which could improve the mechanical properties of the joint. However, the abovementioned researches mainly focused on the metallurgical reaction between the welding heat source and the joint interface, and there were few reports on how to select the interlayer to regulate the steel/magnesium interface.

In this work, aiming at the problem that IMCs could not be formed between Mg and Fe, it was difficult to realize the metallurgical connection between steel and magnesium. The experiments of laser welding were carried out for AZ31B magnesium alloy and DP590 dual-phase steel in an overlapped magnesium-on-steel configuration with interlayer additions. The effects of Al and Sn interlayers on the microstructure and properties of magnesium/steel joints were analyzed, and the reasons for adding interlayers to improve the properties of magnesium/steel joints and the formation mechanism of interface were explored. The selection of interlayer elements was proposed based on the calculation of thermodynamic properties and intrinsic mechanical properties. The research results of this paper provided a theoretical basis for the reasonable selection of interlayer elements in magnesium/ steel welding.

2 Experimental

The experiment materials employed in this work were AZ31B magnesium alloy and DP590 dual-phase steel, and the dimensions of them were $100 \text{ mm} \times 30 \text{ mm} \times 1.4 \text{ mm}$ and $100 \text{ mm} \times 30 \text{ mm} \times 1.5 \text{ mm}$, respectively. The composition is shown in Table 1. Before welding, the base metal was degreased and ground with acetone and gauze

respectively, and the lapped structure of magnesium alloy sheet was placed on the steel sheet for laser welding experiment. Metals Al and Sn were selected as the interlayers and added to the middle of two sheets in the form of powder, as shown in Fig. 1. A YLS-4000-CL fiber laser with a maximum output power of 4 kW and KUKA robot were used for laser welding. The beam parameter product of the fiber laser was 7.2 mm·mrad. The focused laser beam was 0.4 mm in diameter and the wavelength was 1070 nm. When the defocus was zero, the distance from the welding head to the surface of the workpiece was 192 mm. Argon with a flow rate of 15 L/min was used as the protective gas. Taking weld surface quality as the assessment objective, the optimized welding process parameters are shown in Table 2.

Table 1 Composition of welding base material (wt.%)

Material	Al	Zn Mn		Si	С
AZ31B	3.12	0.95	0.15	0.10	-
DP590	0.02	_	1.60	0.0446	0.068
Material	S	P		Fe	Mg
AZ31B	_	_		0.03	Bal.
ALJID				0.03	Dai.

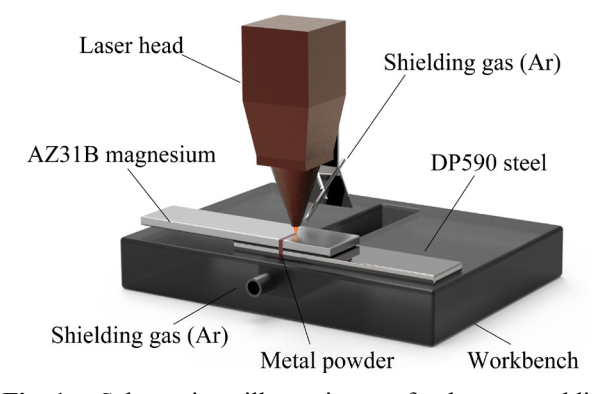


Fig. 1 Schematic illustration of laser welding arrangement

Table 2 Welding parameters used in present work

	01	1	
Laser	Laser	Welding	Flow rate of
power/	defocus/	speed/	Ar gas/
W	mm	$(mm \cdot s^{-1})$	$(L \cdot min^{-1})$
1000	2	30	15
	power/ W	Laser Laser power/ defocus/ W mm	Laser Laser Welding power/ defocus/ speed/ W mm (mm·s ⁻¹)

After welding, the welded joints were cut into small pieces, and the standard metallographic sample preparation steps such as inlaying, grinding and polishing were carried out in sequence. The steel side was etched with nital etchant (4%HNO₃, 96% C₂H₅OH), and the magnesium side was corroded with picric acid solution (15 mL $CH_3COOH + 50 \text{ mL } C_2H_5OH + 3 \text{ g } C_6H_3N_3O_7 +$ 5 mL H₂O). The OLYMPUS DSX510 optical microscope (OM) and Quanta 250 FEG scanning electron microscope (SEM) were used to observe the microstructure of welded joints. The ESCALAB 250 type energy-dispersive X-ray spectrometry (EDS) and Rigaku Rapid IIR type Micro-region X-ray diffraction (micro-XRD) were used to analyze the chemical composition and phase composition of the joint. Specimens for tensile test were prepared according to GB/T6396 - 2008 standards, as shown in Fig. 2. Then, the tensile shear strength of welded joints was tested by CSS-225 universal material testing machine, and the tensile results were taken as the average value of three specimens.

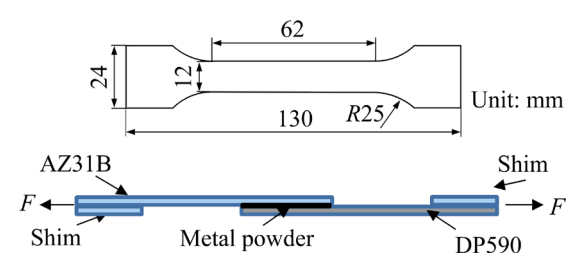


Fig. 2 Sketch of shear-tensile experiment

3 Analysis and discussion

3.1 Surface morphology and mechanical properties of joint

Figure 3 shows the influence of adding interlayer on the surface morphology of magnesium/ steel joints. It can be seen that under the process conditions of laser power of 1000 W, welding speed of 30 mm/s, laser head deflection of 30°, defocusing of +2, and flow of 15 L/min of argon protection. Some defects, such as collapse, edge bite were observed. By contrast, the joint surface was continuous and smooth without spatter as the Al or Sn interlayer was added, and the good formability of weld was presented.

Figure 4 displays the shear performance of magnesium/steel joints. It was found that adding interlayer had a significant effect on joint performance. The maximum load of the joint without adding interlayer was 240 N. With the addition of Sn and Al interlayers, the maximum load of the joint rose to 730 and 590 N, respectively,

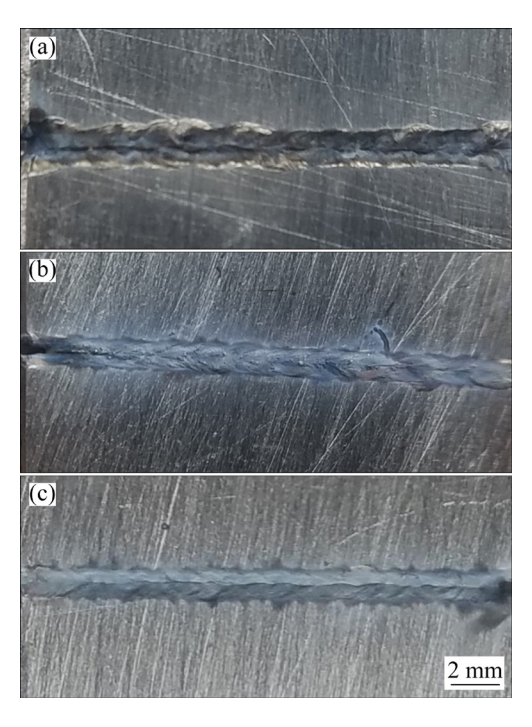


Fig. 3 Surface morphologies of Mg/steel joints with various interlayer: (a) Without interlayer; (b) Al interlayer; (c) Sn interlayer

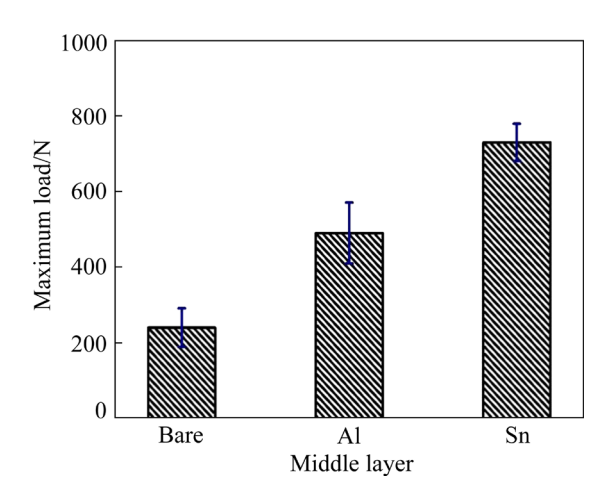


Fig. 4 Maximum load of Mg/steel joints with various interlayers

which was 2.04 times and 1.46 times higher than that without interlayer.

3.2 Microstructure of joint

Figure 5 shows SEM images of joint without interlayer. It can be seen that a small amount of burning loss occurred on steel side, which resulted in defects such as collapse and undercut of the joint (Fig. 5(a)), which was consistent with the results in Fig. 3. Figure 5(b) shows the enlarged red box in Fig. 5(a), no obvious IMCs layer at interface was

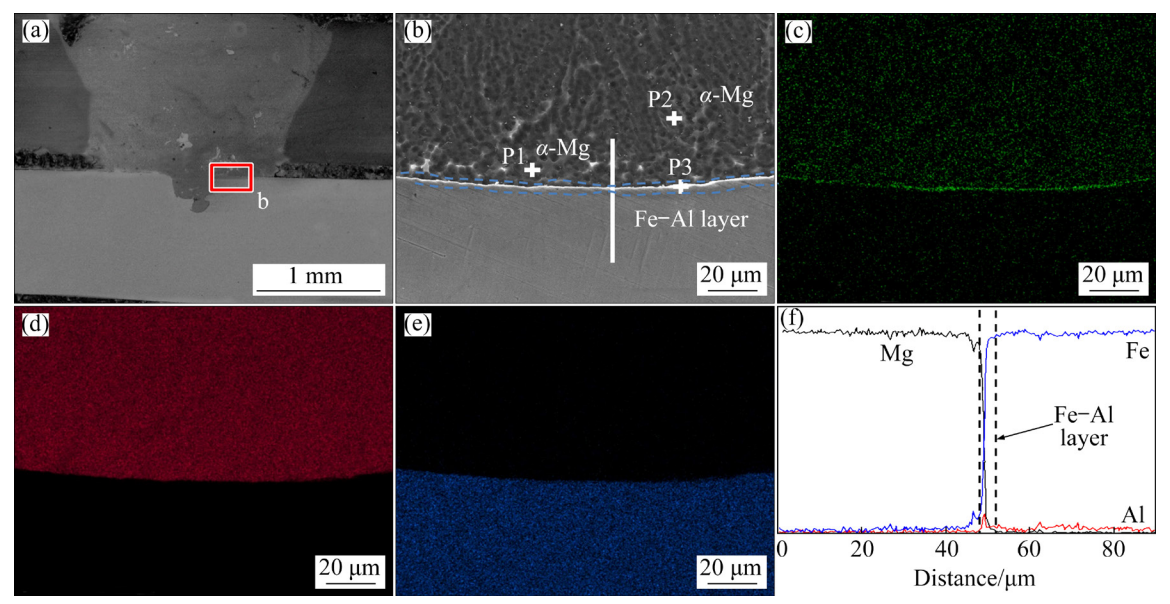


Fig. 5 Element mapping, microstructure and line scanning of Mg/steel joints without interlayer: (a) Cross-section of weld; (b) SEM image of interface; (c) Al element; (d) Mg element; (e) Fe element; (f) Line scanning

found. EDS analysis was performed on the interface layer, and its adjacent areas such as P1, P2 and P3 as shown in Fig. 5(b). The results are shown in Table 3. It can be seen that the main component at P1 and P2 was Mg. The molar ratio of Fe to Al at P3 was about 1:1, which showed that a small amount of Al in magnesium plate and Fe in steel sheet were mixed with each other (Fig. 5(f)). It was speculated that Fe–Al reaction with the thickness of 2 μ m was formed at Fe side interface. LI et al [18] also found that Fe–Al IMCs were formed at interface in the study of magnesium/steel laser brazing with AZ31 brazing filler metal. In order to

Table 3 EDS spot composition analysis results (at.%)

Point	Fe	Ni	Al	Sn	Mg	Possible compound
P1	_	_	1.21	_	96.63	α-Mg
P2	_	_	1.13	_	2.75	α-Mg
P3	49.60	_	46.72	_	3.68	FeAl
P4	_		45.69	_	54.41	$Al_{12}Mg_{17} \\$
P5	33.25	_	64.28	_	2.47	$FeAl_2$
P6	_	_	1.82	_	98.18	α-Mg
P7	_	_	12.18	_	87.82	α-Mg
P8	_	_	7.26		92.74	α-Mg
P9	23.32	74.74	1.92	_	_	$FeSn_3$
P10			1.41	23.87	74.72	$Mg_2Sn+\alpha-Mg$
P11	_	_	1.86	6.47	91.67	α-Mg

further determine the phase structure type of IMCs, XRD analysis was carried out on the joints, and the results are shown in Fig. 6, it was found that FeAl compounds were found at the interface, which was consistent with the results of energy spectrum analysis of the interface layer.

Figure 7 shows SEM images of Al-added joint. The joint was well bound without obvious defects (Fig. 7(a)). EDS analysis results of P5–P8 in Fig. 7(b) are shown in Table 3. It was found that continuous FeAl₂ compound layers were generated at interface on steel side with a thickness greater than 3 μm (Fig. 7(f)), while a discontinuous layer of Mg₁₇Al₁₂ with a thickness of 6–9 μm was formed at interface on magnesium side. XRD results showed that the magnesium/steel interface was composed of

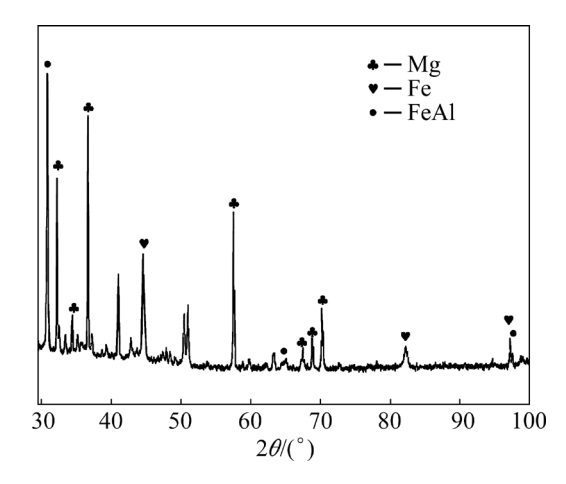


Fig. 6 XRD pattern of Mg/steel joints without interlayer

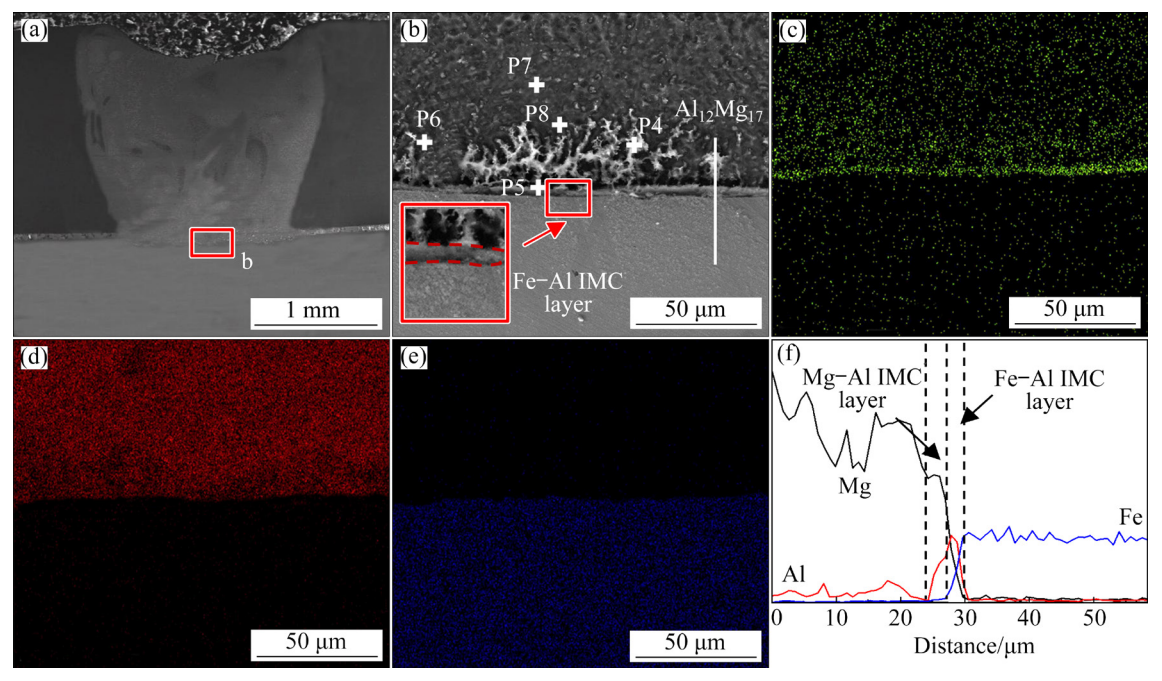


Fig. 7 Elements mapping, microstructure and line scanning of Mg/steel joints with Al interlayer added: (a) Cross-section of weld; (b) SEM microstructure of interface; (c) Al element; (d) Mg element; (e) Fe element; (f) Line scanning

Mg₁₇Al₁₂ and FeAl₂ IMCs (Fig. 8). Therefore, Al metallurgically reacted with Mg and Fe in the joints with the addition of Al interlayer, resulting in the formation of FeAl₂ and the Mg₁₇Al₁₂ compounds on steel and magnesium sides of interface respectively, achieving the metallurgical bonding of magnesium/ steel.

Figure 9 shows the SEM images of Sn-added joint. The joint was well bound and no obvious defects were found (Fig. 9(a)). The EDS analysis results are presented in Table 3, it was found that an greyish-white continuous Fe–Sn compound layer with a thickness of about 4 μ m was formed at

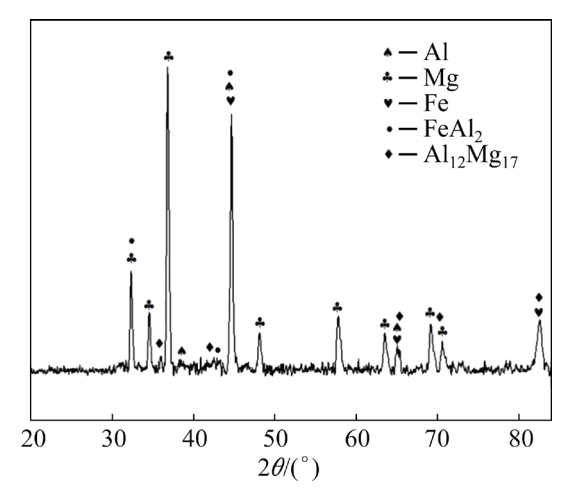


Fig. 8 XRD pattern of Mg/steel joints with Al interlayer

interface on steel side (Fig. 9(b)). The diffusion distance of Sn element to the Mg side was greater than 50 μ m, and a gray mesh-like Mg₂Sn+ α -Mg with eutectoid structure was generated during the reaction uniformly dispersed around the α -Mg matrix. XRD analysis of magnesium/steel joint showed that the interface was composed of Fe₃Sn and Mg₂Sn compounds (Fig. 10). The formation of these new phases was conducive to the metallurgical bonding of the magnesium/steel dissimilar metals.

3.3 Fracture morphology and connection mechanism

Toop model was used to calculate the thermodynamic properties, and the ratio of thermal and shear moduli to bulk moduli (*G/B*) was calculated by first principles. The formation ability and intrinsic mechanical properties of the compound were characterized, and the reasons for the improvement of magnesium/steel joints by adding interlayers were further explained.

The calculation results of thermodynamic properties are shown in Fig. 11. It could be seen that the Gibbs free energy of the compounds formed in the ternary system of Al or Sn with Mg and Fe were all negative values (Figs. 11(a) and (b)), indicating that the addition of the elements Al or Sn

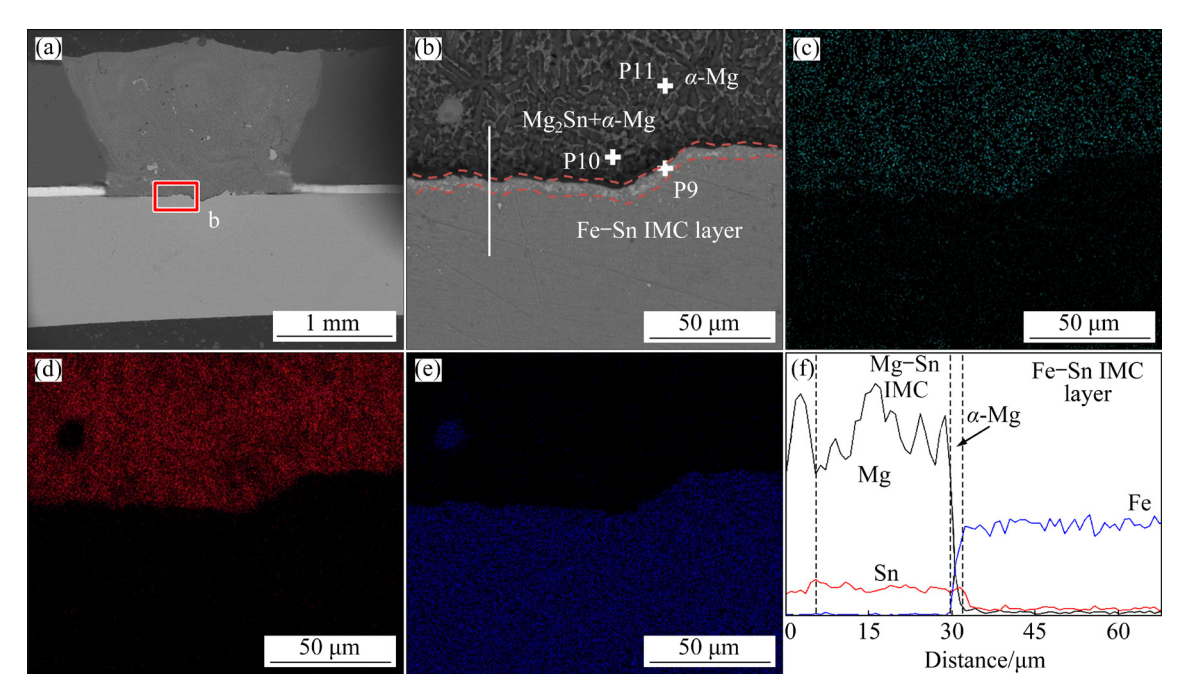


Fig. 9 Elements mapping, microstructure and line scanning of Mg/steel joints with Sn interlayer: (a) Cross-section of weld; (b) SEM microstructure of interface; (c) Al element; (d) Mg element; (e) Fe element; (f) Line scanning

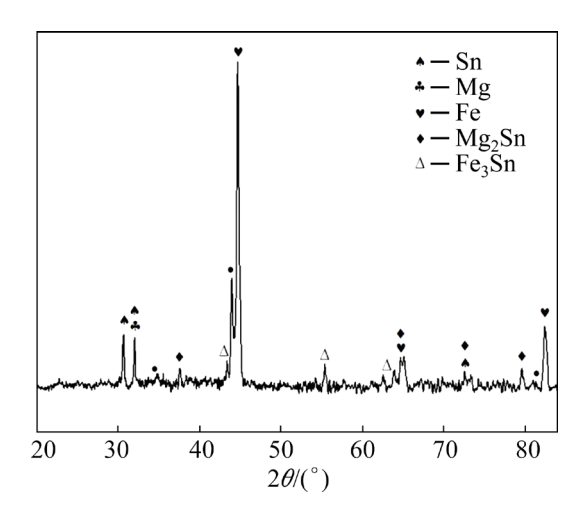


Fig. 10 XRD pattern of Mg/steel joints with Sn interlayer

could react metallurgically with Mg and Fe respectively. The plane projection of three-dimensional surface map was made to obtain its contour map (Figs. 11(c) and (d)). It was found that Gibbs free energy of Mg-Fe-X (X=Al, Sn) ternary system decreased with the increase of Sn and Al content. However, the minimum Gibbs free energy of Mg-Sn-Fe system (G_m=-132.6 kJ/mol) was lower than that of Mg-Al-Fe system ($G_{\rm m}$ =-105.5 kJ/mol). It meant that the system was relatively prone to metallurgical reactions. Generally, the diffusion of elements was essential for the formation of compounds. The lower the chemical potential was, the stronger the driving force of element diffusion was. The chemical potential (μ) of Al in Mg-Al-Fe system (Fig. 11(e)) decreases towards the Fe side, indicating that Al atoms had a tendency to diffuse towards the Fe side, while the chemical potential of Sn in Mg-Sn-Fe system (Fig. 11(f)) decreased towards the Mg side, indicating that Sn tended to diffuse into Mg.

First-principles calculations was performed for the heat of formation and elastic constants of the formed Mg₁₇Al₁₂, Mg₂Sn, FeAl₂ and Fe₃Sn compounds. Figure 12 shows the unit cell diagram of each IMC, where Mg₁₇Al₁₂, Mg₂Sn, and FeAl₂ belong to the tetragonal crystal system, and Fe₃Sn belong to the hexagonal crystal system.

Table 4 listed the calculated results of heat of formation for Mg₁₇Al₁₂, Mg₂Sn, FeAl₂ and Fe₃Sn compounds. Usually, heat of formation was used to characterize the formation ability of compounds. The IMCs could be formed for the negative value of heat of formation, and the greater its negative value, the greater its formative capacity. As could be seen from Table 4, the formation heats of Mg₁₇Al₁₂, Mg₂Sn, FeAl₂ and Fe₃Sn were all negative values, it indicated that these compounds could be formed, which was consistent with the experimental results that these phases were observed at steel/magnesium interface with the addition of Al and Sn interlayer.

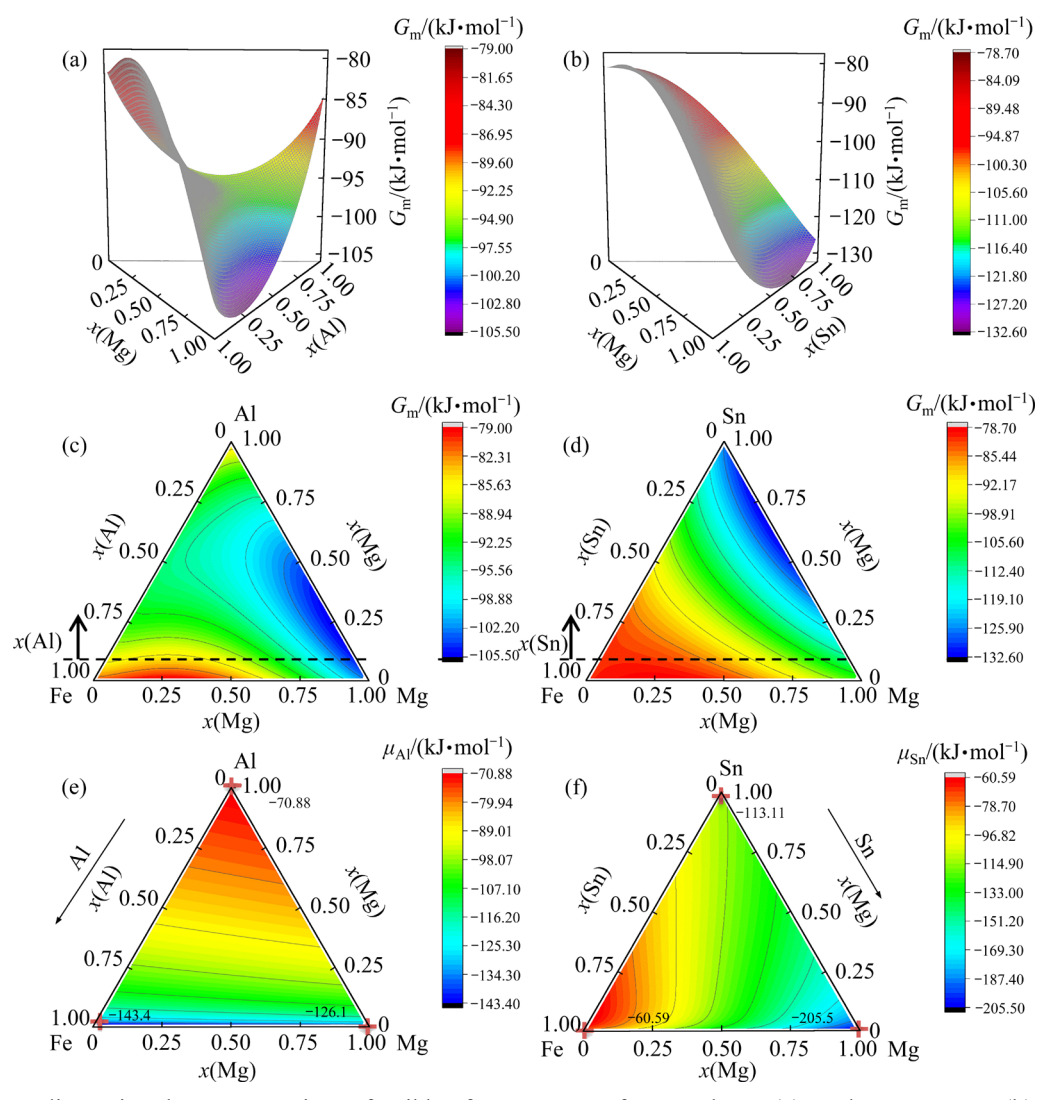


Fig. 11 Three-dimensional representation of Gibbs free energy of Mg–Al–Fe (a) and Mg–Sn–Fe (b) at 1300 K; iso-lines of Gibbs free energy of Mg–Al–Fe (c) and Mg–Sn–Fe (d) ternary systems at 1300 K; chemical potential of Al (e) and Sn (f) in Mg–X–Fe ternary system at 1300 K

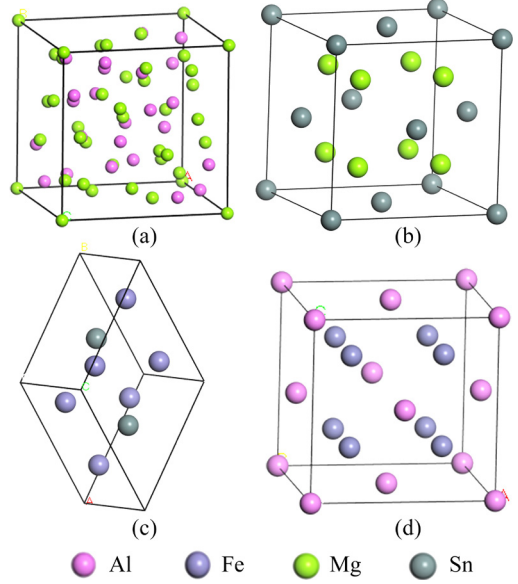


Fig. 12 Crystal structure of $Mg_{17}Al_{12}$ (a), Mg_2Sn (b), Fe_3Sn (c), and $FeAl_2$ (d) phases

Table 4 Heat of formation of Mg₁₇Al₁₂, Mg₂Sn, FeAl₂, and Fe₃Sn phases

DI.	Heat of formation/(kJ·mol ⁻¹)					
Phase	Present	Ref.	Exp.			
$Mg_{17}Al_{12}$	-6.311	-4.64 [19]	-			
Mg_2Sn	-21.538	-20.82 [20]	-24.30 [20]			
$FeAl_2$	-64.427	-57.3 [21]	-59.82 [22]			
Fe_3Sn	-6.183	_	_			

Since Mg₂Sn was more negative than Fe₃Sn in terms of the value of heat formation, it showed that Sn and Mg were prone to form Mg–Sn compounds, while FeAl₂ was more negative than Mg₁₇Al₁₂, it showed that Al and Fe preferred to form Al–Fe compounds, which was consistent with the speculated results in Fig. 11.

					1		
Phase	C11/GPa	C12/GPa	C44/GPa	B/GPa	G/GPa	E/GPa	G/B
Mg_2Sn	68.758	26.183	30.561	40.374	26.851	65.937	0.665
$Mg_{17}Al_{12} \\$	113.145	18.975	31.108	50.365	37.499	90.128	0.745
$FeAl_2$	207.57	100.26	122.35	136.03	94.87	230.93	0.7
Fe ₃ Sn	179.452	112.852	65.725	135.052	52.755	140.031	0.39

Table 5 Elastic constants and moduli of Mg₁₇Al₁₂, Mg₂Sn, FeAl₂ and Fe₃Sn phases

The G/B ratio was used to determine the ductility or brittleness of a phase. When the ratio was less than 0.5, the phase was ductile, otherwise it was the brittle one [23]. The calculation results of G/B values of Mg₁₇Al₁₂, Mg₂Sn, FeAl₂ and Fe₃Sn compounds are shown in Table 5. It could be seen that the G/B values of Mg₂Sn, FeAl₂ and Mg₁₇Al₁₂ (0.665, 0.7 and 0.745) were all greater than 0.5, indicating that these compounds were brittle phases. While the G/B value of Fe₃Sn (0.39) was less than 0.5, indicating that it was ductile phases. Therefore, the compounds formed at interface for magnesium/ steel joint with Al-added were both brittle phases, but the brittleness of FeA12 formed at interface on steel side was lower than that of Mg₁₇Al₁₂ formed on magnesium side. In the case of adding Sn interlayer, formed interface Mg_2Sn at magnesium side was brittle phases, but Fe₃Sn formed on steel side was ductile phases.

Figure 13 shows microhardness distribution across the interfaces with various interlayer. The average hardness of the magnesium base metal and the steel base metal was HV 52 and HV 221, respectively. The hardness increased sharply when it was closing to the Mg/Steel interface, which was caused by the metallurgical reaction at the interface to generate IMC. The hardness of Mg₁₇Al₁₂ formed by the interlayer on the magnesium side of the Al interlayer joint was significantly higher than that of the Mg₂Sn formed by the magnesium side interface of the Sn interlayer joint. Meanwhile, the hardness of FeAl₂ generated at the steel side interface of the Al interlayer joint was also significantly higher than that of Fe₃Sn generated at the steel side interface of the Sn interlayer joint. The hardness analysis results were consistent with the G/B calculation results in Table 5.

Figure 14 displays the fracture morphology of magnesium/steel joints with different interlayers. EDS analysis was performed on the points marked on fracture morphology, and the results are shown

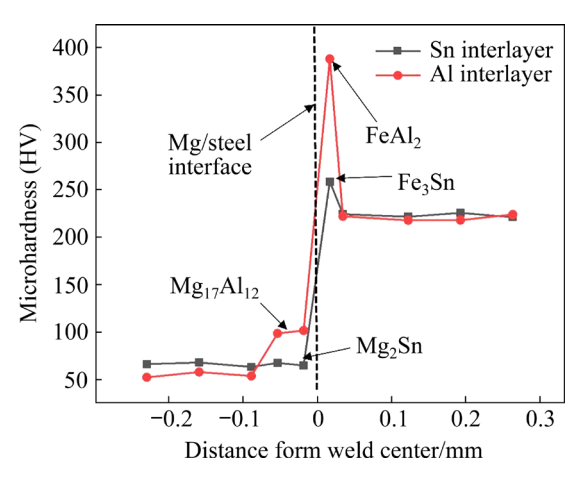


Fig. 13 Microhardness distribution of Mg/steel joints with various interlayers

in Table 6. It could be seen that obvious smooth area contained α-Mg was observed for the fracture of No-added joint (Fig. 14(a)), demonstrating that little metallurgical bonding occurred at magnesium/ steel interface. Meantime, tear ridges appeared at the fracture interface of the joint with adding Al interlayer (Fig. 14(b)). According to the analysis results of EDS, the Mg₁₇Al₁₂ appeared at the interface of the joint was beneficial to improving the joint performance for the metallurgical reaction between Al and Mg. However, there were cleavage steps on the fracture surface. Besides, since the brittleness of Mg₁₇Al₁₂ at interface on magnesium side is greater than that of FeAl₂ on steel side, thus cracks were prone to occur, and the fracture location was on magnesium side. Compared with the two types of joints without interlayer and with Al interlayer, the fracture of the joint interface with Sn interlayer was mainly uneven area with increased laceration ridges and dimples, which was a mixed fracture characteristic of ductile and brittleness. According to the analysis results of EDS, Mg₂Sn compounds were generated at interface. Since Mg₂Sn at interface on magnesium side was a brittle phase, and Fe₃Sn on steel side was a ductile phase, the fracture location was still at interface on magnesium side. As could be seen from the above,

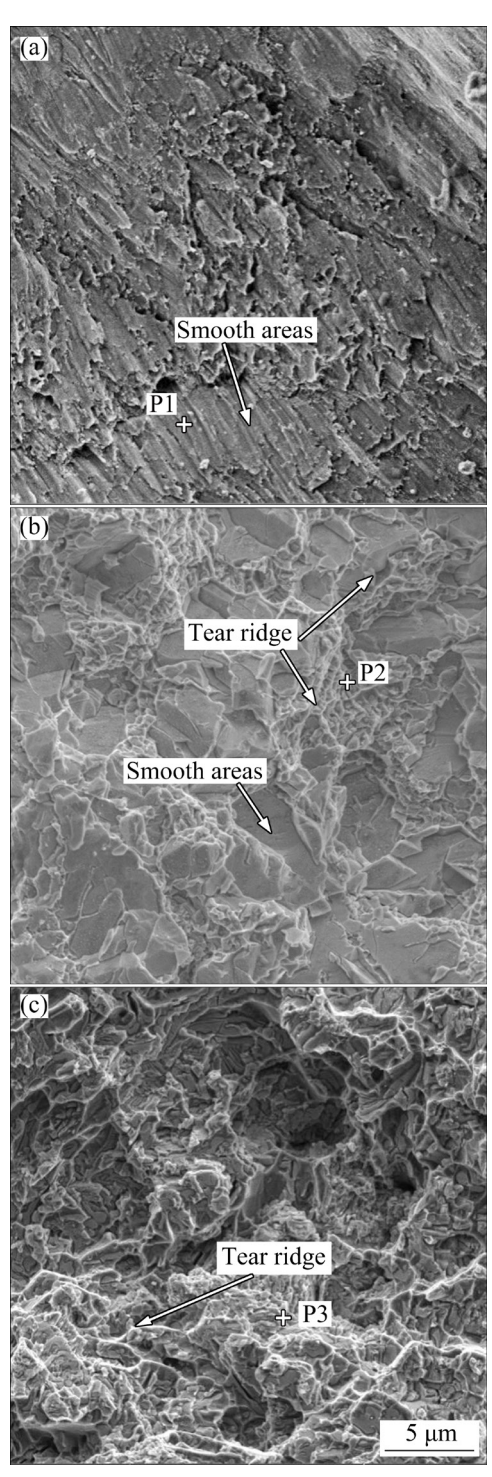


Fig. 14 Fracture morphologies of Mg/steel joints with various interlayers: (a) Bare; (b) Al; (c) Sn

Table 6 EDS spot composition analysis results in Fig. 14 (at.%)

Point	Fe	Ni	Al	Sn	Mg	Possible compound
P1	-	6.78	1.67	-	91.55	α-Mg
P2	_	_	40.42	_	59.58	$Al_{12}Mg_{17} \\$
Р3			1.75	27.37	70.88	$Mg_2Sn+\alpha-Mg$

magnesium/steel metallurgical bonding could be achieved by adding Al and Sn interlayers. However, it was an important factor affecting the properties of magnesium/steel joint for the intrinsic mechanical properties of the compound formed by the metallurgical reaction between the interlayer elements and Mg or Fe.

There was barely solid solution between Fe and Mg, so metallurgical combination of them could not occur. However, the metallurgical combination of magnesium and steel could be realized by adding intermediate interlayer. When selecting intermediate interlayer, the following factors should be considered. First of all, the low Gibbs free energy of interlayer elements in Mg-X-Fe ternary system ensured that the ternary system was prone to metallurgical reaction. Secondly, when the interlayer element reacted with Mg and Fe, the more negative the heat of formation was, the more easily the compound was formed. Finally, according to the intrinsic mechanical properties of the compound formed by the reaction of different interlayer elements with Mg or Fe, if it was a ductile or low-brittle phase, it was beneficial to improve the performance of the steel/magnesium joint. In the ternary system of Mg-X-Fe, the Gibbs free energy of the compounds formed by Sn was lower than that of Al, metallurgical reactions were more likely to occur. In addition, the formation ability of Mg₂Sn generated by the reaction of Sn and Mg was greater than that of Mg₁₇Al₁₂ generated by the reaction of Al and Mg, and the brittleness was lower. In addition, the ductile Fe₃Sn phase could be formed on steel side by the reaction of Sn and Fe. Therefore, compared with Al interlayer, the above considerations were the essential reasons for preferentially choosing Sn as the interlayer element in magnesium/steel welding.

The reaction mechanism between the interlayer Al or Sn element and magnesium/steel interface is shown in Fig. 15. At the laser irradiation, AZ31 magnesium alloy melted immediately, and the interlayer melted through heat conduction. By the combined action of gravity and Marangoni effect, the liquid magnesium merged with the melted interlayer. Meanwhile, the Fe surface was exposed to the liquid metal, so that part of the Fe atoms became active at high temperature. Then Fe atoms diffused at magnesium/steel interface. Since

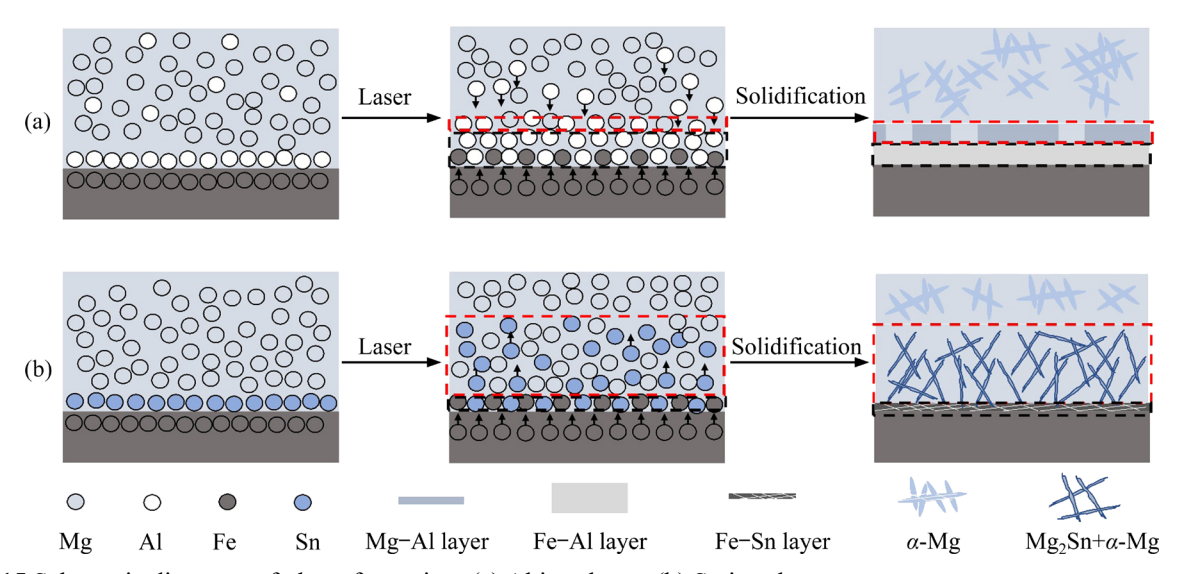


Fig. 15 Schematic diagrams of phase formation: (a) Al interlayer; (b) Sn interlayer

the density of Al was smaller than that of Mg, the density of Sn being larger than that of Mg, Al floated and Sn sunk in molten pool. However, it could be seen that Mg₁₇Al₁₂ was mainly distributed at steel side interface and Mg₂Sn was dispersed at magnesium side interface from the compound distribution in Figs. 7 and 9, which was closely related to the thermodynamic behavior of Sn and Al in the Mg-X-Fe ternary system. According to thermodynamic analysis, Al atoms diffused to the steel side, as a result, the Al atoms on magnesium side transferred to steel side and gathered at interface on steel side (red box in Fig. 15(a)). During the rapid solidification process, eutectic transformation occurred at interface on magnesium side (1), and the steel side interface undergoes an encrustation transformation (2)

$$L \rightarrow \alpha - Mg + \beta - Mg_{17}Al_{12}$$
 (1)

$$L \rightarrow \alpha$$
-Fe+FeAl₂ (2)

From the calculation results of heat of formation, it was well known that it was hard for $Mg_{17}Al_{12}$ to continuously form at interface. Thus, the magnesium/steel joint interface with Al interlayer was constituted with discontinuous $Mg_{17}Al_{12}$ and $FeAl_2$. However, Sn atoms diffused to magnesium side (red box in Fig. 15(b)), and eutectic transformation occurred at magnesium side interface (3), while a small amount of Sn and Fe reacted at interface on steel side (4):

$$L \rightarrow \alpha$$
-Mg+Mg₂Sn (3)

$$L \rightarrow \alpha - Fe + Fe_3Sn + FeSn_2 \tag{4}$$

The diffusion of Sn atoms to magnesium side and the low heat of Mg_2Sn formation make the $Mg_2Sn+\alpha$ -Mg more dispersed at interface on magnesium side.

In summary, without the addition of interlayer, the metallurgical bonding of steel/magnesium could not be achieved, and the mechanical properties of the joint were poor. After adding Al and Sn as interlayers, IMCs such as Mg₁₇Al₁₂ and Mg₂Sn were formed respectively at interface on magnesium side. Meanwhile, FeAl₂ and Fe₃Sn were generated respectively at interface on steel side. By the action of those reactions, the metallurgical connection of magnesium and steel was obtained for improving the joint performance. The mechanical properties of Sn-added joint was higher than that of Al-added. The major reasons for the difference of joint property were as follows: firstly, the weak forming ability of Mg₁₇Al₁₂ and the thermodynamic behavior of Al element in the Mg-Al-Fe ternary system (diffusion to the Fe side) result in the discontinuity of the Mg₁₇Al₁₂ reaction layer at interface, which caused adverse effects on the mechanical properties of the joint. However, Mg₂Sn had a low heat of formation and strong formation ability, and diffused to Mg in the Mg-Al-Fe ternary system. Therefore, the magnesium/steel interface compound was uniformly dispersed in α -Mg so that the joint performance could be improved. In addition, the intrinsic mechanical properties of the compound a critical factor were also affecting improvement of joint performance. Since the brittleness of Mg2Sn was lower than that of Mg₁₇Al₁₂, it was consistent with the analysis of fractures that the Al interlayer joint was brittle fracture, while the Sn interlayer joint was a mixed fracture of ductile and brittleness. The formation of low-brittle compounds was beneficial to improve the performance of steel/magnesium joints.

4 Conclusions

- (1) Under the process conditions of the 1000 W laser power, 30 mm/s welding speed, 30° laser head deflection, 2 mm defocus, and 15 L/min flow rate of argon protection, magnesium/steel metallurgical connection could be realized by adding interlayer. The weld surface was continuous and smooth without spatter, and good surface formability was presented.
- (2) The addition of Sn and Al interlayers for metallurgical reactions with magnesium and steel respectively could significantly improve the mechanical properties of magnesium/steel joints, and the maximum load of the joints were 730 and 590 N, which was 3.04 times and 2.46 times respectively that of the joint without interlayer.
- (3) With the addition of Al interlayer, the brittle Mg₁₇Al₁₂ compound was formed at the joint interface on magnesium side, which limited the further improvement of magnesium/steel joint performance. In the case of adding Sn interlayers, Mg₂Sn with relatively low brittleness was generated at the interface on magnesium side, while Fe₃Sn with ductility was generated on steel side, which was an essential reason that the mechanical properties of magnesium/steel joint with Sn interlayer were higher than those with Al interlayer.

Acknowledgments

The authors are grateful for the financial supports from the National Natural Science Foundation of China (Nos. 51774125, 52174360), and Natural Science Foundation of Hunan Province, China (No. 2020JJ4207).

References

- [1] ATABAKI M M, MA J, LIU W, KOVACEVIC R. Hybrid laser/arc welding of advanced high strength steel to aluminum alloy by using structural transition insert [J]. Materials & Design, 2015, 75(6): 120–135.
- [2] XU Nan, ZHANG Wei-da, CAI Si-qi, ZHOU Ye, SONG Qi-ning, BAO Ye-feng. Microstructure and tensile properties

- of rapid-cooling friction-stir-welded AZ31B Mg alloy along thickness direction [J]. Transactions of Nonferrous Metals Society of China, 2020, 30(12): 3254–3262.
- [3] WANG Xiao-yong, SUN Da-qian. YIN Shi-qiang, LIU Dong-yang. Microstructures and mechanical properties of metal inert-gas are welded Mg-steel dissimilar joints [J]. Transactions of Nonferrous Metals Society of China, 2015, 25(8): 2533–2542.
- [4] ZHANG Zhong-ke, WANG Xi-jing, WANG Pei-chung, ZHAO Gang. Friction stir keyholeless spot welding of AZ31 Mg alloy-mild steel [J]. Transactions of Nonferrous Metals Society of China, 2014, 24(6): 1709–1716.
- [5] TAN Cai-wang, SONG Xiao-guo, MENG Sheng-hao, CHEN Bo, LI Li-qun, FENG Ji-cai. Laser welding-brazing of Mg to stainless steel: Joining characteristics, interfacial microstructure, and mechanical properties [J]. The International Journal of Advanced Manufacturing Technology, 2016, 86(4): 203–213.
- [6] TAN C W, LI L Q, CHEN Y B, NASIRI A M, ZHOU Y. Microstructural characteristics and mechanical properties of fiber laser welded-brazed Mg alloy-stainless steel joint [J]. Welding Journal, 2014, 93(10): 399–409.
- [7] NASIRI A M, WECKMAN D C, ZHOU Y. Interfacial microstructure of diode laser brazed az31b magnesium to steel sheet using a nickel interlayer the formation of a nano-scale Fe(Ni) transition layer on the steel during laser brazing was found to be responsible for the formation of a metallurgical bond between the steel and magnesium [J]. Welding Journal, 2013, 92(1): 1–10.
- [8] TAN C W, CHEN B, SONG X G, ZHOU L, MENG S H, LI L Q, FENG J C. Influence of al interlayer thickness on laser welding of Mg/steel [J]. Welding Journal, 2016, 95(10): 384–394.
- [9] LI Tao-tao, SONG Gang, YU Pei-ni, LIU Li-ming. Interfacial microstructure evolution in fusion welding of immiscible Mg/Fe system [J]. Materials & Design, 2019, 181: 107903.
- [10] TAN Cai-wang, XIAO Li-yuan, LIU Fu-yun, CHEN Bo, SONG Xiao-guo, LI Li-qun, FENG Ji-cai. Influence of laser power on the microstructure and mechanical properties of a laser welded-brazed Mg alloy/Ni-coated steel dissimilar joint [J]. Journal of Materials Engineering and Performance, 2017, 26(6): 2983–2997.
- [11] TAN C W, CHEN Y B, LI L Q, GUO W. Comparative study of microstructure and mechanical properties of laser welded-brazed Mg/steel joints with four different coating surfaces [J]. Science and Technology of Welding and Joining, 2013, 18(6): 466–472.
- [12] NASIRI A M, WECKMAN D C, ZHOU Y. Interfacial microstructure of laser brazed AZ31B magnesium to Sn-plated steel sheet [J]. Welding Journal, 2015, 94(3): 61–72.
- [13] PATEL V K, BHOLE S D, CHEN D L. Characterization of ultrasonic spot welded joints of Mg-to-galvanized and ungalvanized steel with a tin interlayer [J]. Journal of Materials Processing Technology, 2014, 214(4): 811–817.
- [14] LI Li-qun, TAN Cai-wang, CHEN Yan-bin, GUO Wei, HU Xin-bin. Influence of Zn coating on interfacial reactions and

- mechanical properties during laser welding-brazing of Mg to steel [J]. Metallurgical and Materials Transactions A, 2012, 43(12): 4740–4754.
- [15] LIU Li-ming, QI Xiao-dong. Effects of copper addition on microstructure and strength of the hybrid laser-TIG welded joints between magnesium alloy and mild steel [J]. Journal of Materials Science, 2009, 44(21): 5725–5731.
- [16] ZHAO Xiao-ye, TAN Cai-wang, XIAO Li-yuan, XIA Hong-bo, CHEN Bo, SONG Xiao-guo, LI Li-qun, FENG Ji-cai. Effect of the Ni coating thickness on laser welding-brazing of Mg/steel [J]. Journal of Alloys and Compounds, 2018, 769: 1042–1058.
- [17] ZHOU He, LIU Jin-shui, ZHOU Dian-wu, TAO Tao. Effect of Al-foil addition on microstructure and temperature field of laser fusion welded joints of DP590 dual-phase steel and AZ31B magnesium alloy [J]. Transactions of Nonferrous Metals Society of China, 2020, 30(10): 2669–2680.
- [18] LI Li-qun, TAN Cai-wang, CHEN Yan-bin, GUO Wei, SONG Fan. Comparative study on microstructure and mechanical properties of laser welded-brazed Mg/mild steel and Mg/stainless steel joints [J]. Materials & Design, 2013, 43: 59–65.
- [19] HUANG Z W, ZHAO Y H, HOU H, HAN P D. Electronic

- structural, elastic properties and thermodynamics of $Mg_{17}Al_{12}$, Mg_2Si and Al_2Y phases from first-principles calculations [J]. Physica B: Condensed Matter, 2012, 407(7): 1075-1081.
- [20] ZHANG Hui, SHANG Shun-li, SAAL J E, SAENGDEEJING A, WANG Yi, CHEN Long-qing, LIU Zi-kui. Enthalpies of formation of magnesium compounds from first-principles calculations [J]. Intermetallics, 2009, 17(11): 878–885.
- [21] KANG S J, PARK S, KIM M, HAN H N, LEE S K, LEE K Y, KWON Y K. Enhanced mechanical property of Fe-Al alloy due to Mn insertion: ab initio study [J]. Journal of Alloys and Compounds, 2014, 583: 295–299.
- [22] GONZALES-ORMEÑO P G, PETRILLI H M, SCHÖN C G. Ab-initio calculations of the formation energies of BCC-based superlattices in the Fe–Al system [J]. Calphad, 2002, 26(4): 573–582.
- [23] LI Tian, ZHOU Dian-wu, YAN You-rui-ling, PENG Pin, LIU Jin-shui. First-principles and experimental investigations on ductility/brittleness of intermetallic compounds and joint properties in steel/aluminum laser welding [J]. Transactions of Nonferrous Metals Society of China, 2021, 31(10): 2962–2977.

夹层辅助激光焊接镁/钢异种金属的显微组织与性能

陶 韬 1,2, 刘金水 1,2, 周惦武 2, 李会明 2, 王新宇 2

- 1. 湖南大学 材料科学与工程学院,长沙 410082;
- 2. 湖南大学 汽车车身先进设计制造国家重点实验室, 长沙 410082

摘 要:采用镁合金在上、钢板在下且添加中间夹层辅助的激光焊接技术,对 AZ31B 镁合金和 DP590 双相钢平板试件进行焊接,基于热力学性能和本征力学性质的计算来选择夹层元素,分析添加夹层前后镁/钢接头显微组织和性能的变化。结果表明:添加 Sn 和 Al 夹层,接头最大载荷分别为 730 和 590 N,与没有添加夹层相比,分别提高 2.04 倍和 1.46 倍;添加 Al 夹层,接头界面生成脆性较大的 Mg₁₇Al₁₂ 化合物,其限制了镁/钢接头性能提升;而添加 Sn 夹层,界面生成脆性相对较低的 Mg₂Sn 化合物以及延性 Fe₃Sn 化合物,这是添加 Sn 夹层镁/钢接头性能高于添加 Al 夹层的重要原因。

关键词:异种金属焊接;金属间化合物;力学性能;Sn 粉末;Al 粉末

(Edited by Xiang-qun LI)